

Density-Matrix Mean-Field Theory

Junyi Zhang^{1, 2*} and Zhengqian Cheng³

¹ William H. Miller III Department of Physics and Astronomy, Johns Hopkins University,
Baltimore, Maryland 21218, USA

² Institute for Quantum Matter, Johns Hopkins University, Baltimore, Maryland, 21218, USA

³ Department of Applied Physics and Applied Mathematics, Columbia University, New York,
New York 10027, USA

* jzhan312@jhu.edu

January 15, 2024

Abstract

Mean-field theories (MFTs) have proven to be efficient tools for exploring various phases of matter, complementing alternative methods that are more precise but also more computationally demanding. Conventional mean-field theories (MFTs) often fall short in capturing quantum fluctuations, which restricts their applicability to systems characterized by strong quantum fluctuations. In this article, we propose a novel mean-field theory, density-matrix mean-field theory (DMMFT). DMMFT constructs effective Hamiltonians, incorporating quantum environments shaped by entanglements quantified by the reduced density matrices. Therefore, it offers a systematic and unbiased approach to account for effects of fluctuations and entanglements in quantum ordered phases. As demonstrative examples, we show that DMMFT can not only quantitatively evaluate the renormalization of order parameters induced by quantum fluctuations but can even detect the topological order of quantum phases. Additionally, we discuss the extensions of DMMFT for systems at finite temperatures and those with disorders. Our work provides a novel and efficient approach to explore phases exhibiting unconventional quantum orders, which can be particularly beneficial for investigating frustrated spin systems in high spatial dimensions.

Contents

1	Introduction	2
2	Density-Matrix Mean-Field Theory	3
2.1	Conventional Mean-Field Approximation	4
2.2	Density-Matrix Mean-Field Approximation	5
2.3	Comparison of the Mean-Field Approximations	6
3	Applications	7
3.1	Affleck-Kennedy-Lieb-Tasaki Model	8
3.2	Antiferromagnetic Heisenberg Model on Triangular Lattices	9
4	Discussions	11
4.1	Comparisons with Alternative Methods	12
4.2	Systems at Finite Temperatures	13
4.3	Systems with Disorders	13

5 Conclusion	14
A Iterative Algorithm for Mean-Field Equations	15
References	16

1 Introduction

Frustrated Hubbard and Heisenberg models [1–3] have continued to capture research attention over the last half-century due to their potential to host various intriguing quantum phases [4–8], as well as their relevance to high T_c superconductors [9] and their applications in quantum computations [10]. Determining the ground states of frustrated Hubbard and Heisenberg models is often a challenging task.

Exact approaches frequently encounter limitations posed by the exponential wall. In exact diagonalizations (ED), the dimension of the Hilbert space increases exponentially with the system size. In the density-matrix renormalization group (DMRG) [11], the area law provides relief from the exponential wall issue for gapped systems in one spatial dimension ($d = 1$), it still faces exponential scaling challenges for gapless systems or in higher dimensions ($d \geq 2$) [12–14]. On the other hand, quantum Monte Carlo (QMC) methods are less constrained by the system size. Nevertheless, the notorious sign problem often plagues fermionic systems and frustrated magnetic systems [15, 16].

Approximation methods, serving as complements to exact approaches, prove to be useful and efficient tools for exploring various phases of the systems. The usual mean-field theories (MFTs) already provide insights into non-trivial effects arising resulting from the interactions, e.g., the formation of the local moments in metals [17], and the BCS theory for the superconductivity [18]. Conventional MFTs achieve the simplification by neglecting the fluctuations, consequently, they tend to exhibit bias towards ordered states and overlook the nuanced effects stemming from the fluctuations.

Beyond conventional MFTs, various approximations have been proposed for fermionic systems [19–25]. In dynamical mean-field theory (DMFT), a lattice model is mapped to a local impurity model, and the effective action is constructed using Green’s functions as dynamical mean fields [19], which allows DMFT to capture the quantum features of the metal-insulator transitions [20]. While DMFT precisely describes systems in infinite dimensions, the computational demands of solving the local impurity problems with continuous baths necessitate ongoing efforts to further simplify the DMFT. Recently, a quantum embedding method called density matrix embedding theory (DMET) has been introduced to enhance the efficiency of the DMFT by taking the advantage of the frequency-independent local density matrix [21]. More recently, another simplification of DMFT known as variational discrete action theory (VDAT) has also been proposed utilizing sequential product density matrix to variationally determine ground states [22–25].

Despite of the successes of DMFT and its simplifications for fermionic systems, a gap remains in methods beyond semiclassical mean-field approximations for spin systems. Although employing the Holstein-Primakoff transformation [26] allows spins to be mapped to bosons, to which the DMFT may be adapted in principle, the transformation is nonlinear, and the semiclassical large- S expansion becomes less controllable for $S = 1/2$ in the quantum limit, posing challenges for semiclassical methods applied to quantum spins. Similar challenges may be encountered with alternative methods. For instance, in the Schwinger boson representation [27],

one needs to set $\mathcal{N} = 2$ for the quantum limit after a saddle-point mean-field approximation with a large \mathcal{N} .

In this article, we propose a new mean-field method beyond conventional MFTs, which we call density-matrix mean-field theory (DMMFT). DMMFT constructs effective Hamiltonians, incorporating quantum environments shaped by entanglements quantified by the reduced density matrices without presumed semiclassical orders. Therefore, it offers an unbiased approach to account for effects of fluctuations and entanglements in quantum ordered phases. In contrast to QMC and DMFT, DMMFT is generically applicable to systems of fermions, bosons as well as spins, regardless of frustrations. More importantly, by gauging the quantum fluctuations with the reduced DM, DMMFT can detect not only the symmetry-breaking phases in Landau's paradigm but also the topological phases with the help of entanglement spectra. Our work provides a novel and efficient approach to explore phases exhibiting unconventional quantum orders. Particularly, it fills the gap left by the MFTs in studying quantum ordered phases in frustrated spin systems, where semiclassical methods become less controllable in the quantum limit, and QMC methods fail due to the sign problem.

The rest of the article is organized as follows. In Sec. 2, we present the generic formulation of the DMMFT. The mean-field equations of DMMFT are derived in parallel to those of conventional MFTs. Moreover, we demonstrate that DMMFT becomes equivalent to conventional MFTs when the hyperparameter, which gauge the quantum fluctuations, is minimized. In Sec. 3, we apply the DMMFT to two demonstrative examples, 1) the Affleck-Khomoto-Lieb-Tasaki (AKLT) model [28–30], and 2) the antiferromagnetic Heisenberg model on triangular lattices (AFHTL) [31–47]. In the AKLT model, DMFT identifies the topological ground states through their entanglement spectra. In the AFHTL, DMMFT reveals that quantum fluctuations not only renormalize the order parameters but also shift the phase boundaries. In Sec. 4, we compare the DMMFT with the DMRG and the DMFT. Additionally, we discuss the extensions of DMMFT for systems at finite temperatures and those with disorders. Finally, in Sec. 5, we draw conclusions and discuss potential avenues for future research

2 Density-Matrix Mean-Field Theory

In this section, we formulate the DMMFT for a generic Hamiltonian. Let $\mathcal{I} = \{i\}$ be a set of all sites. On each site, there is a collection of local operators $\mathcal{O}_i = \{\mathcal{O}_i^\alpha\}$. A generic Hamiltonian of local operators can be organized as follows

$$H[\mathcal{O}_{\mathcal{I}}] = \sum_{c \in \mathcal{C}} H_c[\mathcal{O}_c] + \sum_{(c,c')} H_{c,c'}[\mathcal{O}_c, \mathcal{O}_{c'}] + \sum_{(c,c',c'')} H_{c,c',c''}[\mathcal{O}_c, \mathcal{O}_{c'}, \mathcal{O}_{c''}] + \dots, \quad (1)$$

where $\mathcal{C} = \{c\}$ is a partition of \mathcal{I} , and $\mathcal{O}_{\mathcal{S}} = \cup_{i \in \mathcal{S}} \mathcal{O}_i$ is the collection of local operators over the sites within a set \mathcal{S} . In Eq.(1), H_c depends only on the local operators within a cluster c , while $H_{c,c'}, H_{c,c',c''}, \dots$ describe the inter-cluster couplings. For systems with finite-range interactions, there are proper partitions such that interactions only involve finitely many clusters.

Now, we formulate the DMMFT for the Hamiltonian in Eq.(1) Since no further assumptions are made specifying the local operators or the microscopic details of the coupling terms, DMMFT is generically applicable to fermions, bosons as well as spins, irrespective of the presence of frustration. In conventional MFTs, a local cluster is separated from the system and coupled to an effective environment, where the environment is assumed to be classical, and the correlated fluctuations between the cluster and the environment are neglected. DMMFT improves the conventional mean-field approximation by including the essential quantum fluctuations in the environment, where the reduced DM is used to gauge the quantum fluctuations and select a Hilbert subspaces approximating the effective environment.

In the following subsections, we will begin by reviewing the conventional mean-field approximation in Sec. 2.1. Then, we will develop the mean-field equations and self-consistency conditions of DMMFT in parallel to those in conventional MFTs in Sec. 2.2. Following this, in Sec. 2.3, we will conduct a comprehensive comparison between the DMMFT and the conventional MFTs. Within this comparison, we will identify a hyperparameter, n_c , that interpolates the DMMFT and the conventional MFTs. Particularly, when n_c attains its minimal value of 1, DMMFT becomes equivalent to the conventional MFTs.

2.1 Conventional Mean-Field Approximation

We review the approximations employed in conventional MFTs before delving into the development of DMMFT. In conventional MFTs, the mean-field decoupling localizes the operator products to individual Hilbert subspaces by neglecting the correlated fluctuations. More precisely, consider an operator product $O_i^\alpha O_j^\beta$ acting on the Hilbert space $\mathcal{H}_i \otimes \mathcal{H}_j$. The conventional mean-field approximation decouples the operator product as follows

$$O_i^\alpha O_j^\beta \approx O_i^\alpha \langle O_j^\beta \rangle + \langle O_i^\alpha \rangle O_j^\beta - \langle O_i^\alpha \rangle \langle O_j^\beta \rangle, \quad (2)$$

where the terms on the right-hand side act on the subspace \mathcal{H}_i or \mathcal{H}_j , or act trivially as an additive c -number. Consequently, the correlated fluctuations $\langle \delta O_i^\alpha \delta O_j^\beta \rangle = \langle O_i^\alpha O_j^\beta \rangle - \langle O_i^\alpha \rangle \langle O_j^\beta \rangle$ vanish in this approximation. Alternatively, from the perspective of the quantum states, as the operator product factorizes in product states, $\langle \phi_i | \otimes \langle \phi_j | O_i^\alpha O_j^\beta | \phi_i \rangle \otimes | \phi_j \rangle = \langle \phi_i | O_i^\alpha | \phi_i \rangle \langle \phi_j | O_j^\beta | \phi_j \rangle$, the conventional MFTs implicitly assume the product structure of the states and neglect quantum entanglements.

Keeping this consideration in mind, we formulate the conventional mean-field approximation for the generic Hamiltonian in Eq.(1) as follows. Given a cluster c , let $\mathcal{C}'_c = \cup c'$ be the collection of the cluster connecting to c , referred to as the environment surrounding c . The associated Hilbert spaces are \mathcal{H}_c and $\mathcal{H}_{\mathcal{C}'_c}$ for the cluster and the environment, respectively, where $\mathcal{H}_{\mathcal{S}} = \otimes_{i \in \mathcal{S}} \mathcal{H}_i$ for a set of sites \mathcal{S} . Retaining the terms within the extended cluster $\bar{c} = c \cup \mathcal{C}'_c$, the local Hamiltonian is

$$\begin{aligned} H[\mathcal{O}_{\bar{c}}] &= H_c[\mathcal{O}_c] + H_{c, \mathcal{C}'_c}[\mathcal{O}_c, \mathcal{O}_{\mathcal{C}'_c}] + H_{\mathcal{C}'_c}[\mathcal{O}_{\mathcal{C}'_c}], \\ H_{c, \mathcal{C}'_c}[\mathcal{O}_c, \mathcal{O}_{\mathcal{C}'_c}] &= \sum_{(c, c'): c' \in \mathcal{C}'_c} H_{c, c'}[\mathcal{O}_c, \mathcal{O}_{c'}] + \sum_{(c, c', c''): c', c'' \in \mathcal{C}'_c} H_{c, c', c''}[\mathcal{O}_c, \mathcal{O}_{c'}, \mathcal{O}_{c''}] + \dots, \\ H_{\mathcal{C}'_c}[\mathcal{O}_{\mathcal{C}'_c}] &= \sum_{c' \in \mathcal{C}'_c} H_{c'}[\mathcal{O}_{c'}] + \sum_{(c', c''): c', c'' \in \mathcal{C}'_c} H_{c', c''}[\mathcal{O}_{c'}, \mathcal{O}_{c''}] + \dots, \end{aligned} \quad (3)$$

where H_c is the Hamiltonian of the focused cluster c , $H_{\mathcal{C}'_c}$ is the Hamiltonian of the environment \mathcal{C}'_c , and H_{c, \mathcal{C}'_c} represents the couplings between the cluster c and its environment \mathcal{C}'_c . If the target state can be approximated by a product state locally, i.e.,

$$|\phi_{\bar{c}}\rangle \approx |\phi_{\bar{c}}^{\text{MF}}\rangle = |\phi_c\rangle \otimes |\phi_{\mathcal{C}'_c}\rangle, \quad (4)$$

a local effective Hamiltonian for the cluster c can be obtained by substituting the operators over $\mathcal{H}_{\mathcal{C}'_c}$ with their expectation values in $|\phi_{\mathcal{C}'_c}\rangle$, i.e.,

$$H_{\text{MF}}^{(c)}[\mathcal{O}_c] = H_c[\mathcal{O}_c] + \langle \phi_{\mathcal{C}'_c} | H_{c, \mathcal{C}'_c}[\mathcal{O}_c, \mathcal{O}_{\mathcal{C}'_c}] | \phi_{\mathcal{C}'_c} \rangle + \langle \phi_{\mathcal{C}'_c} | H_{\mathcal{C}'_c}[\mathcal{O}_{\mathcal{C}'_c}] | \phi_{\mathcal{C}'_c} \rangle, \quad (5)$$

which acts only on the Hilbert subspace \mathcal{H}_c . One solves $|\phi_c\rangle$ as an eigenstate with respect to the effective Hamiltonian $H_{\text{MF}}^{(c)}$ for each cluster c locally. If one further assumes that the target state of the entire system can also be approximated with a product state, i.e.,

$$|\Phi_{\text{MF}}\rangle = \otimes_c |\phi_c\rangle, \quad (6)$$

then, for each extended cluster, $|\phi_{c'}\rangle = \otimes_{c' \in \mathcal{C}'_c} |\phi_{c'}\rangle$. Therefore, Eq.(4), Eq.(5), and Eq.(6) form a closed set of coupled mean-field equations for the conventional MFT.

The mean-field equations can often be further simplified when systems have additional symmetries. If the partition $\mathcal{C} = \{c\}$ respects some symmetry of the system, there exist symmetry transformations relating the clusters $T_{c',c} : c \mapsto c'$. A symmetric mean-field Ansatz state can be constructed simply as $|\Phi_{\text{MF}}\rangle = \otimes_c T_{c,c_0} |\phi_{c_0}\rangle$. Particularly, for a translationally invariant state, all $|\phi_c\rangle$ can be chosen equal to the same state $|\phi_{c_0}\rangle$ in the local Hilbert space \mathcal{H}_{c_0} , then the coupled mean-field equations for the clusters reduce to a single set of self-consistent mean-field equations for $|\phi_{c_0}\rangle$.

The major assumption in the conventional MFTs described above is that the target states can be approximated with product states [Eqs.(4) and (6)], which is, nevertheless, not justified *a priori*. For many ordered states, the correlated fluctuations arising from the quantum entanglements are not negligible, particularly at short range. Prototypically, in frustrated magnetic systems and symmetry-protected topologically ordered systems, such quantum fluctuations and quantum entanglements play essential roles. Improved treatments of quantum fluctuations and quantum entanglements are needed to better understand the emerging quantum ordered phases.

2.2 Density-Matrix Mean-Field Approximation

The simplifications achieved in conventional MFTs stem from the *separability*, i.e., reducing the challenging task of studying the total Hamiltonian H over an exponentially large Hilbert space \mathcal{H}_c to the more manageable tasks of studying the local Hamiltonians $H_{\text{MF}}^{(c)}$ over local \mathcal{H}_c . However, it is not *necessary* for a system to be in a product state for two local subsystems to be separable. The assumptions of the product states [Eqs.(4) and (6)] can thus be relaxed. More precisely, for gapped systems, the correlated fluctuations $\langle \delta O_i^\alpha \delta O_j^\beta \rangle \rightarrow 0$ as $|i-j| \rightarrow \infty$. The absence of long-range entanglements ensures separability, allowing the local physics to be approximated with effective local systems. However, the short-range entanglements encode the quantum fluctuations, demanding a more faithful treatment.

Instead of Eq.(2) for mean-field decoupling, it is instructive to recognize that the entanglement of a local cluster with an (infinite or finitely large) environment can always be *faithfully* reproduced within a finite extension of the cluster. More precisely, consider a generic state $|\Psi\rangle \in \mathcal{H}_c$. The entanglement of the state $|\Psi\rangle$ over the cluster c and the rest parts of the system $\mathcal{C} \setminus c$ can be characterized by the reduced DM

$$\rho_c = \text{Tr}_{\mathcal{C} \setminus c} |\Psi\rangle\langle\Psi|. \quad (7)$$

The entanglement is controlled by \mathcal{H}_c than $\mathcal{H}_{\mathcal{C} \setminus c}$ provided $D_{\mathcal{H}_c} < D_{\mathcal{H}_{\mathcal{C} \setminus c}}$, where $D_{\mathcal{H}}$ denotes the dimension of a Hilbert space \mathcal{H} . According to the purification theorem [48], there exists a state $|\tilde{\Psi}\rangle$ in $\tilde{\mathcal{H}} = \mathcal{H}_c \otimes \tilde{\mathcal{H}}_{\tilde{c}}$ such that $\text{Tr}_{\tilde{c}} |\tilde{\Psi}\rangle\langle\tilde{\Psi}| = \tilde{\rho}_c$ is equivalent to ρ_c , and the dimension of the Hilbert subspace $\tilde{\mathcal{H}}_{\tilde{c}}$ is bounded by $\tilde{D}_{\tilde{c}}^E = \lceil \exp(SE_c) \rceil$, where

$$SE_c = -\text{Tr}_c [\rho_c \ln(\rho_c)], \quad (8)$$

is the entanglement entropy and $\lceil q \rceil$ represents the smallest integer larger than or equal to q . In this context, DMMFT seeks for an effective Hamiltonian $\tilde{H}_{\text{MF}}^{(c)}$ over some $\tilde{\mathcal{H}}$ (to be specified below), such that the reduced DM of the state obtained from the the Hamiltonian,

$$\rho_c^{\text{MF}} = \text{Tr}_{\tilde{c}} |\tilde{\Phi}\rangle\langle\tilde{\Phi}|, \quad (9)$$

well approximates the reduced DM of the target state $\rho_c = \text{Tr}_{\mathcal{C} \setminus c} |\Phi\rangle\langle\Phi|$.

Instead of Eq.(4), DMMFT assumes that *for systems without long-range entanglements*, $\tilde{\mathcal{H}}$ can be found as a Hilbert subspace of $\mathcal{H}_{\bar{c}}$ over the extended cluster \bar{c} . Mathematically, there exists a homomorphism

$$\Pi = \text{Id}_c \otimes \Pi_{\mathcal{C}'_c} : \tilde{\mathcal{H}} \rightarrow \mathcal{H}_{\bar{c}}, \quad (10)$$

and its pseudo-inverse $\Pi^\dagger : \mathcal{H}_{\bar{c}} \rightarrow \tilde{\mathcal{H}}$ is a projector.

To avoid confusion, it is essential to emphasize that the $\tilde{\mathcal{H}}$ constructed in DMMFT differs from that in DMET. The purification theorem only ensures the existence of $\tilde{\mathcal{H}}$ with its dimension bounded by \tilde{D}_c^E from below. In DMET, an optimal \tilde{H} with the lowest possible dimension is employed, but at the cost of a less straightforward construction of the embedding Hamiltonian. In contrast, DMMFT can intuitively construct an effective Hamiltonian by restricting the Hamiltonian for the extended cluster to $\tilde{\mathcal{H}}$, i.e.,

$$\tilde{H}_{\text{MF}}^{(c)}[\mathcal{O}_c, \tilde{\mathcal{O}}_{\mathcal{C}'_c}] = \Pi^\dagger H[\mathcal{O}_{\bar{c}}] \Pi, \quad (11)$$

where the local operators in $\tilde{\mathcal{O}}_{\mathcal{C}'_c}$ are

$$\tilde{\mathcal{O}}_j^\beta = \Pi_{\mathcal{C}'_c}^\dagger O_j^\beta \Pi_{\mathcal{C}'_c}, \forall j \in \mathcal{C}'_c. \quad (12)$$

The reduced density matrix of the target state is approximated with ρ_c^{MF} [Eq.(9)] for an eigenstate $|\tilde{\phi}\rangle$ of $\tilde{H}_{\text{MF}}^{(c)}$.

Reciprocally, for each ρ_c , we may construct the local projectors Π_c as follows. Let $\{|\lambda_i^{(c)}\rangle, |\lambda_i^{(c)}\rangle\}$ be the spectral decomposition of ρ_c , and assume the state vectors are arranged in decreasing order according to their eigenvalues, i.e., $\lambda_i^{(c)} \geq \lambda_j^{(c)}, \forall i < j$. Define

$$\Pi_c = \sum_{i=1}^{n_c} |\lambda_i^{(c)}\rangle \langle \lambda_i^{(c)}|, \quad (13)$$

where $n_c \leq D_{\mathcal{H}_c}$ is a cut-off parameter. For the extended cluster $\bar{c} = c \cup \mathcal{C}'_c$, we choose

$$\Pi_{\mathcal{C}'_c} = \otimes_{c' \in \mathcal{C}'_c} \Pi_{c'}. \quad (14)$$

Parallel to the mean-field equations for the conventional MFTs, Eqs.(9) – (14) constitute a closed set of coupled mean-field equations for the DMMFT. The procedures for implementing the DMMFT algorithm are outlined in Appendix A. In the presence of symmetries, the mean-field equations can be further simplified. Specifically, for a translationally invariant target state $|\Phi\rangle$, the reduced DMs of the local clusters are all identical to the same reduced DM ρ_{c_0} (as are the projectors). Consequently, the coupled mean-field equations for the clusters reduce to a single set of self-consistent mean-field equations for ρ_{c_0} .

2.3 Comparison of the Mean-Field Approximations

Comparing conventional MFTs with DMMFT, we find the cut-off parameter n_c in Eq.(13) can be regarded as a hyperparameter interpolating the DMMFT and the conventional MFT. To demonstrate this point, we first observe that when $D_{\mathcal{H}_{\mathcal{C}'_c}} = 1$, DMMFT is equivalent to a conventional MFT. If the ground state is a product state [Eq.(6)], the local reduced density matrix of cluster c is $\rho_c = |\phi_c\rangle \langle \phi_c|$. The expectation values of the local observables agree

$$\langle O_i^\alpha \rangle_c = \langle \phi_c | O_i^\alpha | \phi_c \rangle = \text{Tr}_c(\rho_c O_i^\alpha). \quad (15)$$

Moreover, since $\Pi = \text{Id}_c \otimes (\otimes_{c'} |\phi_c\rangle\langle\phi_c|)$, $\tilde{\mathcal{H}}$ is isomorphic to \mathcal{H}_c , and the effective Hamiltonians $\tilde{H}_{\text{MF}}^{(c)}$ are $H_{\text{MF}}^{(c)}$ identical under this isomorphism.

Furthermore, from Eq.(14), we have $D_{\mathcal{H}_{c'}} = \prod_{c' \in \mathcal{C}'_c} n_{c'}$. Therefore, we may take n_c as a hyperparameter interpolating the conventional MFT and the DMMFT. When $n_c = 1$ (set to its minimal value), the DMMFT simply reduces to the conventional MFT, which underestimates the quantum fluctuations. When $n_c = D_{\mathcal{H}_c}$ (set to its maximal value), the DMMFT describes a collection of (overlapped) extended cluster \bar{c} , which overestimate the quantum fluctuations compared to the infinite system in the thermodynamic limit. Therefore, as n_c increases from 1 to $D_{\mathcal{H}_c}$, more and more quantum fluctuations are included.

Since n_c gauges the amount of quantum fluctuations included in DMMFT from underestimation to overestimation, it seems reasonable to expect an optimal choice of its value, which leads to the following *conjecture*.

Conjecture. *The optimal choice of the hyperparameters is given by*

$$n_c^* = \tilde{D}_c^E = \lceil \exp(SE_c) \rceil. \quad (16)$$

We do not have a mathematical proof of this conjecture, which nevertheless will not harm the practicality of the DMMFT. Particularly, one may take $n_c = \tilde{D}_c^E$ as a rule-of-thumb choice and treat n_c as a *variational* hyperparameter.

It is easy to observe that ρ_c generically has non-vanishing entanglement entropy whenever $D_{\mathcal{H}_{c'}} > 1$. This is exactly the short-range entanglement captured by the DMMFT beyond the conventional MFTs. Not surprisingly, one expects that the DMMFT may detect short-range entangled topological phases with a properly chosen n_c . In Sec. 3.1, we demonstrate with the AKLT model that DMMFT can correctly detect the topological ground states in terms of the entanglement spectra without being biased to the symmetry-breaking states.

Lastly, we comment on the separability in DMMFT. In contrast to Eq.(6) for the conventional MFTs, DMMFT does not assume the product structure of the state. Instead, the weaker version of the separability adopted by DMMFT is

$$\rho_{c_1, c_2}^{(2)} = \text{Tr}_{\mathcal{C} \setminus (c_1 \cup c_2)} |\Phi\rangle\langle\Phi| \approx \rho_{c_1} \otimes \rho_{c_2}, \quad (17)$$

for any two clusters c_1 and c_2 that are not connected.

3 Applications

In this section, we apply the DMMFT to two demonstrative examples, the AKLT model and the AFHTL. These two models have been extensively studied in the literatures (cf. Ref. 28–47 and the references therein). The AKLT model is an exactly solvable model with topological ground states, despite the vanishing semiclassical (symmetry breaking) order parameters [29, 30]. On the other hand, the AFHTL represents a prototypical model for frustrated magnetism. With only nearest neighbor couplings and easy axis anisotropy, the AFHTL is known to order in a three-sublattice ordered state homologous to the semiclassical Néel state. However, the quantum fluctuations play non-trivial roles in stabilizing the ordered state [45–47] and significantly renormalize the order parameter [31]. In Sec. 3.1, we demonstrate that DMMFT can correctly detect the topological ground states based on the entanglement spectra. In Sec. 3.2, we compare the phases of the AFHTL in an external magnetic field determined by DMMFT and conventional MFT.

3.1 Affleck-Kennedy-Lieb-Tasaki Model

We apply the DMMFT to the AKLT model. The AKLT model is a one-dimensional spin-1 chain defined by the Hamiltonian

$$H_{\text{AKLT}} = \sum_i P_{i,i+1}^{(S=2)} = \sum_i \frac{1}{2} [\mathbf{S}_i \cdot \mathbf{S}_{i+1} + \beta (\mathbf{S}_i \cdot \mathbf{S}_{i+1})^2 + \gamma], \quad (18)$$

where β describes the biquadratic coupling and γ is an additive constant, \mathbf{S}_i are spin-1 operators whose representations in the S^z -basis are

$$S_i^x = \frac{1}{\sqrt{2}} \begin{pmatrix} 0 & 1 & 0 \\ 1 & 0 & 1 \\ 0 & 1 & 0 \end{pmatrix}, S_i^y = \frac{1}{\sqrt{2}} \begin{pmatrix} 0 & -i & 0 \\ i & 0 & -i \\ 0 & i & 0 \end{pmatrix}, S_i^z = \begin{pmatrix} 1 & 0 & 0 \\ 0 & 0 & 0 \\ 0 & 0 & -1 \end{pmatrix}. \quad (19)$$

The coefficients β and γ are determined by the condition that each term in the Hamiltonian is a projector to the Hilbert subspace of total spin $S = 2$. More precisely, when $\beta = 1/3$, and $\gamma = 2/3$,

$$P_{i,i+1}^{(S=2)}(x) = \frac{1}{2}(x + \beta x^2 + \gamma) = \begin{cases} 1, & x = 1, \\ 0, & x = -1, -2. \end{cases} \quad (20)$$

where $x = \mathbf{S}_i \cdot \mathbf{S}_{i+1} = 1, -1, -2$ in total spin sectors $\mathcal{H}_{\{i,i+1\}}^{(S=2,1,0)}$ respectively. By construction, H_{AKLT} describes antiferromagnetic nearest neighbor couplings penalizing only on neighboring spins being in $S = 2$ states.

The AKLT model is an exactly solvable system, showcasing non-trivial topological order. Notably, it features spin-1/2 (fractional to spin-1) edge states and exhibits 4-fold degeneracy of the ground states for an open chain. This makes the AKLT model a valuable benchmark example.

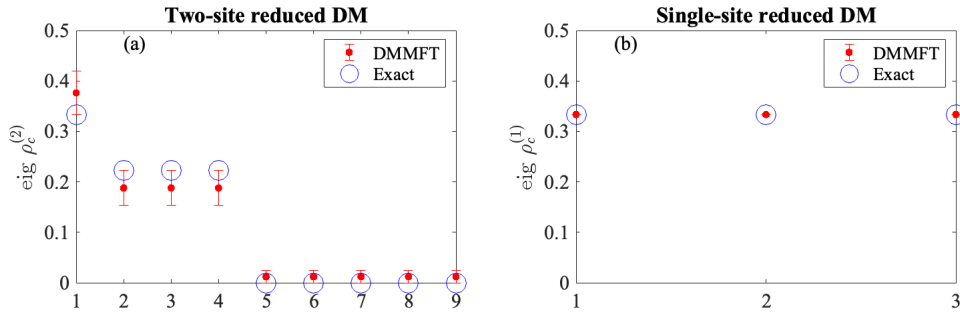


Figure 1: Spectra of the two-site and single-site reduced DMs for the AKLT model. Blue circles denote exact values, while red dots with error bars represent DMMFT results.

Let us consider a two-site cluster c situated in the bulk of an infinite chain. By translational symmetry, any two-site cluster c within the chain shares the same reduced DM $\rho_c^{(2)}$. The spectrum of the two-site reduced DM is exactly known and given by $\text{eig} \rho_c^{(2)} = \{\frac{1}{3}, \frac{2}{9}, \frac{2}{9}, \frac{2}{9}, 0, 0, 0, 0, 0\}$. Furthermore, if we trace out one of the sites within the cluster, we obtain the single-site reduced DM whose spectrum is exactly known, $\text{eig} \rho_c^{(1)} = \{\frac{1}{3}, \frac{1}{3}, \frac{1}{3}\}$.

We apply the DMMFT to the AKLT model, focusing the two-site cluster c and solving the reduced DM $\rho_c^{(2)}$ self-consistently according to the mean-field equations as described in Sec. 2.2. Specifically, the reduced DM is calculated over an extended cluster encompassing the left and

right nearest neighboring two-site clusters to c . The associated Hilbert space is denoted as $\mathcal{H}_c = \mathcal{H}_l \otimes \mathcal{H}_c \otimes \mathcal{H}_r$, where $\mathcal{H}_{l,r} \sim \Pi_c(\mathcal{H}_c)$ are the Hilbert subspaces selected by the reduced DM, as per Eq.(13). We choose the cut-off parameter $n_c = 4$.

In Fig. 1, the spectra of the two-site and single-site reduced DMs are presented. Blue circles represent exact values, while red dots depict DMMFT results. The spectrum of the two-site reduced DM obtained with the DMMFT reasonably aligns with the exact values [Fig. 1(a)], notably capturing the correct degeneracies. The entanglement entropy of the two-site cluster evaluated by DMMFT is $SE_{c,\text{MF}}^{(2)} = 1.58$. Although it is slightly larger than the exact value $SE_{c,\text{exact}}^{(2)} = 1.3689$, this discrepancy is expected due to the cut-off parameter n_c chosen being marginally larger than $\exp(SE_{c,\text{exact}}^{(2)}) = 3.9310$. Fig. 1(b) displays the spectrum of the single-site reduced DM, where the DMMFT results align excellently with the exact values. The single-site entanglement entropy $SE_c^{(1)} = 1.0986 = \ln(3)$ also matches. Furthermore, the expectation values of two spins within the cluster $\langle S_{1,2}^\alpha \rangle = \text{Tr}_c(S_{1,2}^\alpha \rho_c)$ both vanish. This implies that the ground states found by DMMFT are not biased towards the semiclassical Néel states, which agrees with the exact results.

3.2 Antiferromagnetic Heisenberg Model on Triangular Lattices

We apply the DMMFT to another illustrative example, the AFHTL. The Hamiltonian for the AFHTL involving nearest neighbor anisotropic exchange interactions is given by

$$\begin{aligned} H_{AFH} &= \sum_{i,j} \left[J_{xy} \left(S_i^x S_j^x + S_i^y S_j^y \right) + J_z S_i^z S_j^z \right] \\ &= \sum_{i,j} J \left[\mathcal{A} \left(S_i^x S_j^x + S_i^y S_j^y \right) + S_i^z S_j^z \right], \end{aligned} \quad (21)$$

where J_z and J_{xy} are strengths of longitudinal and transverse exchange interactions. For antiferromagnetic couplings, it is more convenient to parameterize the model with $J = J_z > 0$ and $\mathcal{A} = J_{xy}/J_z$. The phases of the system only depend on the dimensionless parameter \mathcal{A} that specifies the exchange anisotropy. Our focus is on the easy-axis case, i.e., $0 \leq \mathcal{A} \leq 1$. The two limiting points of \mathcal{A} are: 1) $\mathcal{A} = 0$, where the transverse exchange terms vanish (often referred to as the Ising limit), and 2) $\mathcal{A} = 1$, where the exchange interactions have full rotational symmetry (often referred to as the Heisenberg limit). Both of the limits have been extensively studied in the literatures. Particularly, in the Ising limit, quantum fluctuations are additionally introduced by the transverse magnetic field, and the sign problem of the diagonal (longitudinal) frustrations can be mitigated in the QMC simulations [47, 49]; while in the Heisenberg limit the system orders in the so-called 120° -Néel state, as confirmed by various numerical methods [31–33, 41, 42].

While the phase diagram is believed to be bounded by the Ising and Heisenberg limits for a generic anisotropy parameter $0 < \mathcal{A} < 1$, computing the details of quantum phases becomes challenging, particularly due to the QMC sign problem when $\mathcal{A} \neq 0$. A study in Ref. 42 utilized large-size cluster mean-field theory (belonging to the class of conventional MFTs) with a scaling scheme, which provides a reasonable benchmark for the quantum phase diagram. With DMMFT, we can more efficiently and quantitatively capture the effects of quantum fluctuations with a small cluster of three sublattice sites.

For illustrative purposes, we focus on the phases of the AFHTL with easy-axis anisotropy subjected to a longitudinal external field, i.e.,

$$H_{AFH,Z} = H_{AFH} + H_Z, \quad (22)$$

where $H_Z = -\sum_i g \mu_B h_z S_i^z$ is the Zeeman coupling of the spins to the magnetic field h_z . In

our DMMFT calculations, we set the gyromagnetic factor $g\mu_B = 1$ and h_z is measured in the corresponding natural unit.

Four phases emerge in the AFHTL with generic easy-axis anisotropy under a longitudinal external field. They are the coplanar “Y”-shaped phase, the collinear up-up-down (UUD) phase, the coplanar “V”-shaped phase, and the collinear polarized phase in the order of increasing h_z . All these phases are compatible with a cluster partition of three-sublattice sites and translational symmetries. A simple order parameter distinguishing these phases is the magnetization along the easy axis, i.e.,

$$M_c^z = \sum_{\alpha \in c} S_\alpha^z = S_A^z + S_B^z + S_C^z, \quad (23)$$

where the subscript $\alpha = A, B, C$ labels three sublattice sites within the cluster c . The polarized and the UUD phases are characterized by magnetization plateaux at $M_c^z = M_z^{c,(s)}$ and $M_c^z = M_z^{c,(s)}/3$, respectively, where $M_z^{c,(s)} = \frac{3}{2}$ is the saturation magnetization. The “V”-shaped phase is sandwiched in between the UUD and the polarized phases, while the “Y”-shaped phase appears at low fields. A distinguishing order parameter characterizing the non-collinearity of the “Y”-shaped phase is the vector chirality

$$\kappa_V = \frac{8}{3\sqrt{3}} (\mathbf{S}_A \times \mathbf{S}_B + \mathbf{S}_B \times \mathbf{S}_C + \mathbf{S}_C \times \mathbf{S}_A), \quad (24)$$

where the normalization factor is chosen such that $|\kappa_V| = 1$ for the 120° -Néel state of $S = \frac{1}{2}$ spins without being renormalized by quantum fluctuations.

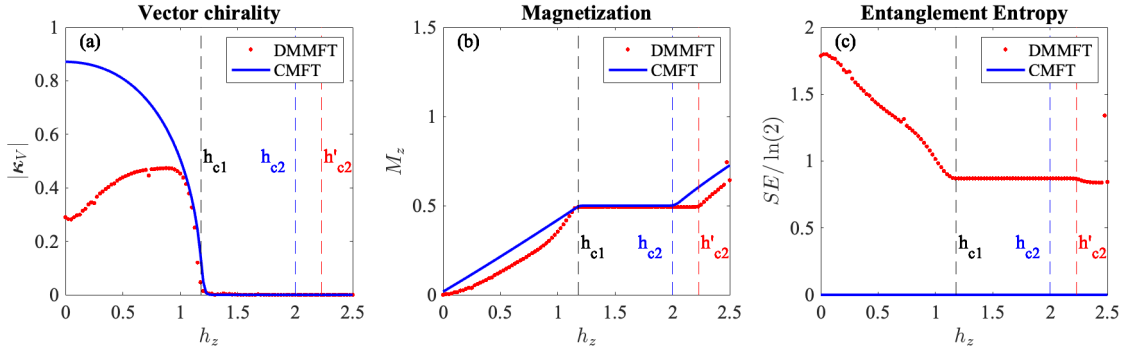


Figure 2: Phase diagram of AFHTL in a longitudinal magnetic field ($\mathcal{A} = 0.9$). (a) Vector chirality. (b) Magnetization. (c) Entanglement Entropy. Red dots represent DMMFT results, while blue curves depict conventional mean-field theory (CMFT) results. Vertical dashed lines indicate phase boundaries. h_{c1} distinguishes the “Y”-shaped phase from the UUD phase, where DMMFT and CMFT are in agreement. h_{c2} distinguishes the UUD-shaped phase from the “V”-shaped phase. Determined from the magnetization curves, the value of h_{c2} in blue from CMFT exhibits a discernible difference compared to h_{c2}' in red from DMMFT.

In our DMMFT calculations, we choose an extended cluster \bar{c} comprising of four three-sublattice clusters with periodic boundary conditions. Utilizing periodic boundary conditions is to minimize the boundary effects, since the Hilbert subspaces selected by the reduced DM is sensitive to the boundary conditions as known in DMRG [50]. While all four phases are homologous to their corresponding semiclassical ordered states, the quantum fluctuations play crucial roles in the “Y”-shaped and UUD phases. Specifically, quantum fluctuations lift the

accidental degeneracies in the semiclassical ground state manifold, which is known as quantum order-by-disorder [45, 46], and significantly renormalize the magnitudes of the ordered spins [31–33].

In Fig. 2 we present the dependence of the vector chirality, the magnetization, and the entanglement entropy of the ground states of AFHTL (with anisotropy parameter $\mathcal{A} = 0.9$) on the longitudinal magnetic field, calculated with the DMMFT (red) and the conventional MFT (blue). The cut-off parameter n_c , as discussed in Sec. 2.3 interpolating the conventional MFT and the DMMFT, is set to $n_c = 4$ for the DMMFT and $n_c = 1$ for the conventional MFT.

In Fig. 2(a), the vector chirality calculated with conventional MFT decreases monotonically as h_z increases in the “Y”-shaped phase and vanishes in the UUD and the “V”-shaped phases. In sharp contrast, the vector chirality calculated with DMMFT, does not decrease monotonically in the “Y”-shaped phase. Notably, the vector chirality at $h_z = 0$ in DMMFT is only about 30% of that in conventional MFT. The discrepancy reflects the renormalization of the ordered spins due to the quantum fluctuations. Examining the magnitude of the ordered spins more closely, we find $|\langle \mathbf{S} \rangle| = 0.269 \pm 0.014$ for small anisotropy $\mathcal{A} = 0.9$. This value is only about 50% of $S = \frac{1}{2}$ but agrees with the expectation from previous reported values [31–33]. Since κ_V scales as S^2 , a reduction factor of about 25% is expected for the magnitude of the vector chirality at $h_z = 0$. The curves of the DMMFT and the conventional MFT converge as h_z increases and both vanish beyond h_{c1} (the critical field separating the “Y”-shaped and the UUD phases determined according to the magnetization curves). With stronger h_z , the spins are aligned closer to the easy axis, and the effect of the quantum fluctuations weakens, which is clearly evidenced from the monotonically decreasing entanglement entropy in the “Y”-shaped phase as shown in Fig. 2(c). Therefore, the suppression of the quantum fluctuations and the aligning of the spins towards the collinear UUD configuration by the longitudinal magnetic field jointly lead to the non-monotonic dependence of the vector chirality $|\kappa_V|$ on h_z .

As h_z surpasses h_{c2} , the system transitions towards the “V”-shaped phase, deviating from the $\frac{1}{3}$ magnetization plateau of the UUD phase. Fig. 2(b) demonstrates a discernible difference in the critical field determined from the magnetization curves in DMMFT (h'_{c2}) and in conventional MFT (h_{c2}). Notably, the range of the field stabilizing the UUD phase in DMMFT is larger than that in conventional MFT. Although the UUD configuration is homologous to the semiclassical correspondence, quantum fluctuations aid in stabilizing the UUD phase [42]. Especially in the Heisenberg limit, the UUD phase is only stable at one point of $h_z = h_{c2} = \frac{1}{3}h_z^{(s)} = 1.5$ (where $h_z^{(s)}$ is the saturation field) in the classical phase diagram, while it extends to a finite range of the field in the quantum phase diagram. A similar effect of quantum fluctuations is also expected when $\mathcal{A} < 1$. Since n_c used in DMMFT is larger than that in conventional MFT, more quantum fluctuations are included, a larger field range ($h'_{c2} > h_{c2}$) that stabilizes the UUD phase is expected.

Additionally, a self-consistency check for the choice of $n_c = 4$ in DMMFT can be confirmed from the entanglement entropy in the “Y”-shaped phase. At $h_z = 0$, we have $SE_c \approx 1.8 \ln(2)$. Therefore, $\tilde{D}_c^E = \lceil \exp(SE_c) \rceil = 4$.

4 Discussions

In Sec. 4.1, we undertake a comparative analysis of DMMFT with DMRG and DMFT. Additionally, in Sec. 4.2, we extend the DMMFT for systems at finite temperatures, and in Sec. 4.3, we extend the DMMFT for systems with disorders.

4.1 Comparisons with Alternative Methods

We first compare DMMFT with DMRG. The constructions of the effective Hamiltonian appear similar, where the reduced DM is employed to select Hilbert subspace significant with respect to the target state. The resemblance between the DMMFT and the infinite DMRG is most pronounced when the spatial dimension $d = 1$ as illustrated in the AKLT model in Sec. 3.1. The primary difference lies in where the Hilbert space $\tilde{\mathcal{H}} = \mathcal{H}_c \otimes \tilde{\mathcal{H}}_c$ is chosen. In DMMFT, the projector $\Pi_{c'}$ is iteratively optimized solely over the Hilbert space $\mathcal{H}_{c'}$ without changing the cluster size of the environment. Conversely, in infinite DMRG, the environment is constructed iteratively over the Hilbert space of the semi-infinite chains. Gauged by the quantum entanglement, the dimension of the Hilbert subspace selected for constructing the effective Hamiltonian is bounded by \tilde{D}_c^E [Eq.(16)] in both cases. As \tilde{D}_c^E is bounded by the size of the cluster c , DMRG can feasibly select a finite significant Hilbert subspace without being hindered by the infinite size of the environment asymptotically. On the contrary, in DMMFT, we assume that the significant Hilbert subspace resides within $\mathcal{H}_{c'}$, which is a reasonable approximation, especially for short-range entangled systems. Ignoring practical constraints provided we choose the cluster size being larger than the typical entanglement range. the DMMFT and the DMRG are equivalent in $d = 1$.

The advantages of DMMFT become more significant in higher dimensions, $d \geq 2$. In DMRG, a d -dimensional system is compactified to a quasi-one-dimensional system, and an artificial one-dimensional chain of clusters winds through the system. Consequently, even in the case of a short-range entangled system, artificial long-range entanglements emerge for sites physically close but distant along the chain. In contrast, DMMFT makes use of the separability [Eq.(17)] enables the study of local problems over extended clusters without introducing artificial long-range entanglements arising from the transverse dimensions. From this perspective, DMMFT may be regarded as a mean-field approximation of DMRG and proves particularly valuable for short-range entangled systems in higher dimensions.

Now, we turn to compare DMMFT with DMFT. In DMFT, designed for fermionic systems, the effective action is constructed over a local cluster, employing the single-particle Green's function as a dynamical mean-field to capture fluctuations [19, 20]. This local problem, entailing a dynamical mean-field, is subsequently mapped to an effective impurity model and solved using ED or QMC kernels [19]. In contrast to the Anderson impurity model tailored for fermions, establishing a comparable impurity model for spins is not a straightforward task. Furthermore, even if a spin impurity model aligned with the principles of DMFT could be formulated, the challenge persists in efficiently solving it. Constructing a generic spin impurity (if not impossible) can introduce significant frustrations, which leads to the failure of the QMC kernel due to the sign problem. On the other hand, achieving an accurate representation of the environment requires incorporating a large number of spins beyond those in the local cluster, which causes the ED kernel to rapidly encounter the exponential wall. A simplification of DMFT proposed in DMET for fermionic systems involves utilizing the local density matrix, a static observable, instead of the dynamical Green's function [21]. While a formal generalization of DMET to spin systems is feasible, the challenge lies in identifying a suitable reference wave-function that facilitates straightforward Schmidt decomposition and the construction of the embedding Hamiltonian. On the contrary, in DMMFT, the reduced density matrix is generally defined for many-body states, making DMMFT naturally applicable to fermions, bosons, as well as spins.

An alternative approach to investigating the ground state of a quantum many-body system is to work directly with the wave function. One example can be the Gutzwiller method, which uses Gutzwiller wave-function as an variational Ansatz [51–54]. The Gutzwiller approximation can be viewed as a quantum embedding approach in a unified perspective with DMFT and DMET [55]. More recently, VDAT has been proposed to solve the shortcomings of

Gutzwiller Approximation and simplify the computational complexity of DMFT. In VDAT, the variational ansatz is the sequential product density matrix, which is evaluated via the discrete action theory [22, 23]. The VDAT Ansatz is controlled by an integral parameter \mathcal{N} , and it is asymptotically exact as \mathcal{N} tends to infinity but also becomes more computationally demanding. While it has been demonstrated that VDAT can yield accurate ground state wave functions for fermionic systems, even with \mathcal{N} as small as 3 [24, 25], it faces challenges when applied to spin systems. Constructing the sequential product density matrix for the spin system is straightforward; however, the absence of Wick's theorem for spin systems presents a challenge in efficiently applying discrete action theory to evaluate the Ansatz.

Integrating wave function approaches with DMMFT raises the question of determining a global state from reduced density matrices of local clusters. This challenge is recognized as the quantum marginal problem [56]. Finding a general solution to this problem is currently beyond the scope of this paper and remains an open and challenging research question [57].

4.2 Systems at Finite Temperatures

The extension of DMMFT for systems at finite temperatures is straightforward. In Eq.(9), we use the ground state of the effective Hamiltonian over the extended cluster to compute the reduced DM. At finite temperatures, assuming local thermal equilibrium, we can average the reduced DMs of the eigenstates weighted by the Boltzmann distribution. Specifically, let $\{E_\alpha, |\tilde{\phi}_\alpha\rangle\}$ be the eigensystems of $\tilde{H}_{\text{MF}}^{(c)}$. Then, the thermally averaged reduced DM is given by

$$\begin{aligned} [\rho_c^{\text{MF}}]_T &= \sum_\alpha w_\alpha \rho_c^\alpha, \\ w_\alpha &= \frac{\exp[-E_\alpha/(k_B T)]}{\sum_\beta \exp[-E_\beta/(k_B T)]}, \\ \rho_c^\alpha &= \text{Tr}_{\tilde{c}}[|\tilde{\phi}_\alpha\rangle\langle\tilde{\phi}_\alpha|], \end{aligned} \quad (25)$$

where k_B is the Boltzmann constant, and the square bracket with a subscript T indicates the thermal average. As discussed in Sec. 2.3, when $D_{\mathcal{H}_{c'_c}} = 1$, DMMFT reduces to the CMFTs at zero temperature. It is straightforward to check that, since $[\rho_c^{\text{MF}}]_T \sim \exp[-\tilde{H}_{\text{MF}}^{(c)}/(k_B T)]$ when $D_{\mathcal{H}_{c'_c}} = 1$, the extension of DMMFT according Eq.(25) also aligns with the conventional MFTs at finite temperatures.

However, it is worth noting that the thermal averaging in Eq.(25) does not fully capture all thermal fluctuations. Specifically, at low temperatures, it is often the gapless long wave length modes (Goldstone modes) that dominate the thermal fluctuations. However, due to the mean-field approximation inherent in DMMFT, these thermal fluctuations are neglected. Therefore, similar to all other mean-field methods, DMMFT tends to underestimate the impact of thermal fluctuations at finite temperatures.

4.3 Systems with Disorders

Disorders are an inevitable aspect of experiments. Even minuscule amounts of disorders can alter the nature of fragile quantum phases, particularly in the frustrated systems. Consequently, it becomes crucial to incorporate disorders into the DMMFT framework.

In the presence of the disorders, the Hamiltonian of the extended cluster undergoes direct modification, denoted as

$$H[\mathcal{O}_{\tilde{c}}] \rightarrow H^{(\delta)}[\mathcal{O}_{\tilde{c}}], \quad (26)$$

where the superscript δ labels the types of the disorders. However, the process of averaging over disorders is more intricate than the thermal average discussed in Sec. 4.2.

Consider a straightforward scenario involving a single magnetic vacancy in the cluster c , wherein there can be either no vacancies or one vacancy on a site $i \in c$. In this case, we denote $\delta \in \Delta = \{0\} \cup c$, where $\delta = 0$ signifies no vacancies in the cluster c . We assume the probability measure of the disorder configurations to be $P_\Delta(\delta)d\delta$. Analogous to to Eq.(25), it is intuitive to to define an average over the disorders as

$$\begin{aligned} [\rho_c^{\text{MF}}]_{\Delta, \text{ann}} &= \int_{\Delta} \rho_c^{(\delta)} P_\Delta(\delta) d\delta, \\ \rho_c^{(\delta)} &= \text{Tr}_z |\tilde{\phi}_{(\delta)}\rangle \langle \tilde{\phi}_{(\delta)}|, \end{aligned} \quad (27)$$

where $\tilde{\phi}_{(\delta)}$ is the ground state of the effective Hamiltonian $\tilde{H}_{\text{MF}}^{(c),(\delta)}$, and the square bracket with a subscript Δ indicates the average over the disorder configurations. The physical meaning of $[\rho_c^{\text{MF}}]_{\Delta, \text{ann}}$ so-defined requires further clarification. When $[\rho_c^{\text{MF}}]_{\Delta, \text{ann}}$ is employed to set the effective environment $C'_c = \{c'\}$ for the cluster c , each c' is already averaged over various disorder configurations according to Eq.(27). In other words, the disorders are *annealed*. For this reason, we also add the subscript “ann” in Eq.(27).

In experiments, magnetic vacancies often exhibit behavior more akin to static disorders than fluctuating disorders, particularly when the vacancies are not thermally migrating. Disorders as such are often referred to as *quenched* disorders, in contrast to the annealed disorders. In this case, we consider all possible disorder configurations over the extended cluster \bar{c} . Assume \bar{c} consisting of ν simple clusters, including the focused cluster c and $\nu - 1$ clusters in the environment. If the simple clusters are identical, all possible disorder configurations of the quenched disorders form a set $\Delta = \Delta^\nu = (\delta_1, \delta_2, \dots, \delta_\nu)$. We obtain coupled mean-field equations for $\{\rho_c^{(\delta)}\}_\Delta$. Once $\{\rho_c^{(\delta)}\}_\Delta$ is solved, the expectation values of local observables averaged over the quenched disorders should be calculated as

$$[\langle O_i^\alpha \rangle]_{\Delta, \text{quen}} = \int_{\Delta} \text{Tr}_c [O_i^\alpha \rho_c^{(\delta)}] P_\Delta(\delta) (d^\nu \delta), \quad (28)$$

where $P_\Delta(\delta)(d^\nu \delta)$ is the probability measure over the configuration space of the quenched disorders Δ . In the special case where each vacancy is independent and subjected to an identical distribution $P_\Delta(\delta)d\delta$, then $P_\Delta(\delta)(d^\nu \delta) = \prod_{n=1}^\nu P_\Delta(\delta_n)d\delta_n$.

In real systems, the effects of disorders can be more complicated. For instance, there can be vacancies clusters due to lower formation free energy, and the probability measure of the vacancies no longer takes a simple product form. Moreover, disorders can manifest as inhomogeneity of the samples, especially when scale of the probe is small, and the effects of disorders are not self-averaged in the experiments. Despite of the complications of disorders arising in real systems, DMMFT can, in principle, be adapted to include the disorder effects accordingly.

5 Conclusion

In this study, we introduce a novel mean-field approach, DMMFT, specifically designed to capture quantum fluctuations beyond conventional MFTs. Combining the strengths of DMRG and DMFT, DMMFT stands out as an efficient and unbiased method applicable to fermions, bosons, and spins, even in the presence of frustrations. A noteworthy feature of DMMFT is its ability to discern topological phases, a capability further enhanced by its utilization of the reduced density matrix. Additionally, DMMFT seamlessly extends to systems at finite temperatures and with disorders. In conclusion, DMMFT provides an effective tool for exploring phases exhibiting unconventional quantum orders, particularly beneficial for investigating frustrated spin systems in high spatial dimensions.

Acknowledgements

This work is supported as part of the Institute for Quantum Matter, an Energy Frontier Research Center funded by the U.S. Department of Energy, Office of Science, Office of Basic Energy Sciences, under Award DESC0019331. This work is also partially supported by the NSF CAREER Grant DMR-1848349. JYZ is additionally supported by TIPAC from the Department of Physics and Astronomy, Johns Hopkins University. ZC is supported by the Columbia Center for Computational Electrochemistry. JYZ acknowledges motivating discussions with Collin Broholm, Oleg Tchernyshyov, and Tong Chen. JYZ also thanks Salvia Felixsen Skogen for the hospitality at Domini Katzen Institute.

A Iterative Algorithm for Mean-Field Equations

In Section 2.2, we established a closed set of coupled mean-field equations for DMMFT, delineated by Eqs. (9) to (14). Here, we present an iterative algorithm, as outlined in Table 1, to achieve self-consistent solutions numerically.

Step number	Step description
0	Initialize a set of trial reduced DMs $\{\rho_c\}_{c \in \mathcal{C}}$.
For each cluster c :	
1	Diagonalize ρ_c , and construct Π_c according to Eq.(13).
2	Use Eq.(14) to construct $\Pi_{c'}$.
3	Use Eq.(10) to construct Π .
4	Use Eq.(11) to construct $\tilde{H}_{\text{MF}}^{(c)}$.
5	Diagonalize $\tilde{H}_{\text{MF}}^{(c)}$ and select the target state $ \tilde{\phi}_c\rangle$.
6	Calculate new ρ_c according to Eq.(9).
0'	Use new $\{\rho_c\}_{c \in \mathcal{C}}$ to update the trial reduced DMs, and repeat steps 1 - 6 until convergence.

Table 1: DMMFT implementation steps.

There remain some noteworthy considerations. In Step 0, while a stable self-consistent solution should be independent of initial values, providing an initial guess close to the self-consistent solution often aids convergence. An empirical approach is to start with a trivial ρ_c that can be constructed from solutions of conventional MFTs. In Step 0', a linear interpolation of the reduced DM

$$\rho_c^{(n+1)} = (1 - \alpha)\rho_c^{(n)} + \alpha\rho_c^{(n,\text{new})}, \quad (29)$$

can be employed for updating ρ_c . Here, $\rho_c^{(n)}$ represents the reduced DM used in Step 0 at the n -th iteration, and $\rho_c^{(n,\text{new})}$ is the new reduced DM obtained in Step 0'. The learning rate α varies in the range (0, 1). Larger values of α lead to a more rapid update, while smaller values contribute to stabilizing the iterative process.

Finally, the hyperparameter n_c used in Eq.(13) in Step 1 can be compared to $\tilde{D}_c^E = \lceil \exp(SE_c) \rceil$, where the entanglement entropy is calculated according to Eq.(8). It is important to note that setting $n_c = 1$ should recover the results of conventional MFTs.

Funding information JYZ is supported by IQM EFRC DOE under Award DESC0019331, NSF CAREER under Grant DMR-1848349, and TIPAC PHA JHU. ZC is supported by the Columbia

Center for Computational Electrochemistry.

References

- [1] L. Balents, *Spin liquids in frustrated magnets*, Nature **464**(7286), 199 (2010), doi:[10.1038/nature08917](https://doi.org/10.1038/nature08917).
- [2] M. J. P. Gingras and P. A. McClarty, *Quantum spin ice: a search for gapless quantum spin liquids in pyrochlore magnets*, Reports on Progress in Physics **77**(5), 056501 (2014), doi:[10.1088/0034-4885/77/5/056501](https://doi.org/10.1088/0034-4885/77/5/056501).
- [3] C. Broholm, R. J. Cava, S. A. Kivelson, D. G. Nocera, M. R. Norman and T. Senthil, *Quantum spin liquids*, Science **367**(6475), eaay0668 (2020), doi:[10.1126/science.aay0668](https://doi.org/10.1126/science.aay0668), <https://www.science.org/doi/pdf/10.1126/science.aay0668>.
- [4] P. W. Anderson, *Resonating valence bonds: A new kind of insulator?*, Mater. Res. Bull. **8**, 153 (1973), doi:[10.1016/0025-5408\(73\)90167-0](https://doi.org/10.1016/0025-5408(73)90167-0).
- [5] P. W. A. P. Fazekas, *On the ground state properties of the anisotropic triangular antiferromagnet*, Philos. Mag. **30**, 423 (1974), doi:[10.1080/14786439808206568](https://doi.org/10.1080/14786439808206568).
- [6] V. Kalmeyer and R. B. Laughlin, *Equivalence of the resonating-valence-bond and fractional quantum hall states*, Phys. Rev. Lett. **59**, 2095 (1987), doi:[10.1103/PhysRevLett.59.2095](https://doi.org/10.1103/PhysRevLett.59.2095).
- [7] A. Kitaev, *Anyons in an exactly solved model and beyond*, Annals of Physics **321**(1), 2 (2006), doi:<https://doi.org/10.1016/j.aop.2005.10.005>, January Special Issue.
- [8] C. Castelnovo, R. Moessner and S. L. Sondhi, *Magnetic monopoles in spin ice*, Nature **451**, 42 (2008), doi:[10.1038/nature06433](https://doi.org/10.1038/nature06433).
- [9] P. W. Anderson, *The resonating valence bond state in La_2CuO_4 and superconductivity*, Science **235**(4793), 1196 (1987), doi:[10.1126/science.235.4793.1196](https://doi.org/10.1126/science.235.4793.1196), <https://www.science.org/doi/pdf/10.1126/science.235.4793.1196>.
- [10] A. Kitaev, *Fault-tolerant quantum computation by anyons*, Annals of Physics **303**(1), 2 (2003), doi:[https://doi.org/10.1016/S0003-4916\(02\)00018-0](https://doi.org/10.1016/S0003-4916(02)00018-0).
- [11] S. R. White, *Density matrix formulation for quantum renormalization groups*, Phys. Rev. Lett. **69**, 2863 (1992), doi:[10.1103/PhysRevLett.69.2863](https://doi.org/10.1103/PhysRevLett.69.2863).
- [12] H. C. Jiang, Z. Y. Weng and D. N. Sheng, *Density matrix renormalization group numerical study of the kagome antiferromagnet*, Phys. Rev. Lett. **101**, 117203 (2008), doi:[10.1103/PhysRevLett.101.117203](https://doi.org/10.1103/PhysRevLett.101.117203).
- [13] S. Yan, D. A. Huse and S. R. White, *Spin-liquid ground state of the $s = 1/2$ kagome Heisenberg antiferromagnet*, Science **332**(6034), 1173 (2011), doi:[10.1126/science.1201080](https://doi.org/10.1126/science.1201080), <https://www.science.org/doi/pdf/10.1126/science.1201080>.
- [14] Z. Zhu, P. A. Maksimov, S. R. White and A. L. Chernyshev, *Topography of spin liquids on a triangular lattice*, Phys. Rev. Lett. **120**, 207203 (2018), doi:[10.1103/PhysRevLett.120.207203](https://doi.org/10.1103/PhysRevLett.120.207203).
- [15] G. Senatore and N. H. March, *Recent progress in the field of electron correlation*, Rev. Mod. Phys. **66**, 445 (1994), doi:[10.1103/RevModPhys.66.445](https://doi.org/10.1103/RevModPhys.66.445).

- [16] A. W. Sandvik, *Computational Studies of Quantum Spin Systems*, AIP Conference Proceedings **1297**(1), 135 (2010), doi:[10.1063/1.3518900](https://pubs.aip.org/aip/acp/article-pdf/1297/1/135/11407753/135_1_online.pdf), https://pubs.aip.org/aip/acp/article-pdf/1297/1/135/11407753/135_1_online.pdf.
- [17] P. W. Anderson, *Localized magnetic states in metals*, Phys. Rev. **124**, 41 (1961), doi:[10.1103/PhysRev.124.41](https://doi.org/10.1103/PhysRev.124.41).
- [18] J. Bardeen, L. N. Cooper and J. R. Schrieffer, *Theory of superconductivity*, Phys. Rev. **108**, 1175 (1957), doi:[10.1103/PhysRev.108.1175](https://doi.org/10.1103/PhysRev.108.1175).
- [19] A. Georges, G. Kotliar, W. Krauth and M. J. Rozenberg, *Dynamical mean-field theory of strongly correlated fermion systems and the limit of infinite dimensions*, Rev. Mod. Phys. **68**, 13 (1996), doi:[10.1103/RevModPhys.68.13](https://doi.org/10.1103/RevModPhys.68.13).
- [20] G. Kotliar, S. Y. Savrasov, K. Haule, V. S. Oudovenko, O. Parcollet and C. A. Marianetti, *Electronic structure calculations with dynamical mean-field theory*, Rev. Mod. Phys. **78**, 865 (2006), doi:[10.1103/RevModPhys.78.865](https://doi.org/10.1103/RevModPhys.78.865).
- [21] G. Knizia and G. K.-L. Chan, *Density matrix embedding: A simple alternative to dynamical mean-field theory*, Phys. Rev. Lett. **109**, 186404 (2012), doi:[10.1103/PhysRevLett.109.186404](https://doi.org/10.1103/PhysRevLett.109.186404).
- [22] Z. Cheng and C. A. Marianetti, *Variational discrete action theory*, Phys. Rev. Lett. **126**, 206402 (2021), doi:[10.1103/PhysRevLett.126.206402](https://doi.org/10.1103/PhysRevLett.126.206402).
- [23] Z. Cheng and C. A. Marianetti, *Foundations of variational discrete action theory*, Phys. Rev. B **103**, 195138 (2021), doi:[10.1103/PhysRevB.103.195138](https://doi.org/10.1103/PhysRevB.103.195138).
- [24] Z. Cheng and C. A. Marianetti, *Precise ground state of multiorbital mott systems via the variational discrete action theory*, Phys. Rev. B **106**, 205129 (2022), doi:[10.1103/PhysRevB.106.205129](https://doi.org/10.1103/PhysRevB.106.205129).
- [25] Z. Cheng and C. A. Marianetti, *Gauge constrained algorithm of variational discrete action theory at $\mathcal{N} = 3$ for the multiorbital hubbard model*, Phys. Rev. B **108**, 035127 (2023), doi:[10.1103/PhysRevB.108.035127](https://doi.org/10.1103/PhysRevB.108.035127).
- [26] T. Holstein and H. Primakoff, *Field dependence of the intrinsic domain magnetization of a ferromagnet*, Phys. Rev. **58**, 1098 (1940), doi:[10.1103/PhysRev.58.1098](https://doi.org/10.1103/PhysRev.58.1098).
- [27] D. P. Arovas and A. Auerbach, *Functional integral theories of low-dimensional quantum Heisenberg models*, Phys. Rev. B **38**, 316 (1988), doi:[10.1103/PhysRevB.38.316](https://doi.org/10.1103/PhysRevB.38.316).
- [28] F. D. M. Haldane, *Nonlinear field theory of large-spin Heisenberg antiferromagnets: Semiclassically quantized solitons of the one-dimensional easy-axis néel state*, Phys. Rev. Lett. **50**, 1153 (1983), doi:[10.1103/PhysRevLett.50.1153](https://doi.org/10.1103/PhysRevLett.50.1153).
- [29] I. Affleck, T. Kennedy, E. H. Lieb and H. Tasaki, *Rigorous results on valence-bond ground states in antiferromagnets*, Phys. Rev. Lett. **59**, 799 (1987), doi:[10.1103/PhysRevLett.59.799](https://doi.org/10.1103/PhysRevLett.59.799).
- [30] I. Affleck, T. Kennedy, E. H. Lieb and H. Tasaki, *Valence bond ground states in isotropic quantum antiferromagnets*, Communications in Mathematical Physics **115**(3), 477 (1988).
- [31] D. A. Huse and V. Elser, *Simple variational wave functions for two-dimensional Heisenberg spin- $\frac{1}{2}$ antiferromagnets*, Phys. Rev. Lett. **60**, 2531 (1988), doi:[10.1103/PhysRevLett.60.2531](https://doi.org/10.1103/PhysRevLett.60.2531).

- [32] T. Jolicoeur, E. Dagotto, E. Gagliano and S. Bacci, *Ground-state properties of the $s=1/2$ Heisenberg antiferromagnet on a triangular lattice*, Phys. Rev. B **42**, 4800 (1990), doi:[10.1103/PhysRevB.42.4800](https://doi.org/10.1103/PhysRevB.42.4800).
- [33] S. R. White and A. L. Chernyshev, *Néel order in square and triangular lattice Heisenberg models*, Phys. Rev. Lett. **99**, 127004 (2007), doi:[10.1103/PhysRevLett.99.127004](https://doi.org/10.1103/PhysRevLett.99.127004).
- [34] Z. Zhu and S. R. White, *Spin liquid phase of the $s = \frac{1}{2} J_1 - J_2$ Heisenberg model on the triangular lattice*, Phys. Rev. B **92**, 041105 (2015), doi:[10.1103/PhysRevB.92.041105](https://doi.org/10.1103/PhysRevB.92.041105).
- [35] W.-J. Hu, S.-S. Gong, W. Zhu and D. N. Sheng, *Competing spin-liquid states in the spin- $\frac{1}{2}$ Heisenberg model on the triangular lattice*, Phys. Rev. B **92**, 140403 (2015), doi:[10.1103/PhysRevB.92.140403](https://doi.org/10.1103/PhysRevB.92.140403).
- [36] Y. Iqbal, W.-J. Hu, R. Thomale, D. Poilblanc and F. Becca, *Spin liquid nature in the Heisenberg $J_1 - J_2$ triangular antiferromagnet*, Phys. Rev. B **93**, 144411 (2016), doi:[10.1103/PhysRevB.93.144411](https://doi.org/10.1103/PhysRevB.93.144411).
- [37] A. Wietek and A. M. Läuchli, *Chiral spin liquid and quantum criticality in extended $s = \frac{1}{2}$ Heisenberg models on the triangular lattice*, Phys. Rev. B **95**, 035141 (2017), doi:[10.1103/PhysRevB.95.035141](https://doi.org/10.1103/PhysRevB.95.035141).
- [38] S. Hu, W. Zhu, S. Eggert and Y.-C. He, *Dirac spin liquid on the spin-1/2 triangular Heisenberg antiferromagnet*, Phys. Rev. Lett. **123**, 207203 (2019), doi:[10.1103/PhysRevLett.123.207203](https://doi.org/10.1103/PhysRevLett.123.207203).
- [39] S.-S. Gong, W. Zheng, M. Lee, Y.-M. Lu and D. N. Sheng, *Chiral spin liquid with spinon fermi surfaces in the spin- $\frac{1}{2}$ triangular Heisenberg model*, Phys. Rev. B **100**, 241111 (2019), doi:[10.1103/PhysRevB.100.241111](https://doi.org/10.1103/PhysRevB.100.241111).
- [40] Y.-F. Jiang and H.-C. Jiang, *Nature of quantum spin liquids of the $s = \frac{1}{2}$ Heisenberg antiferromagnet on the triangular lattice: A parallel dmrg study*, Phys. Rev. B **107**, L140411 (2023), doi:[10.1103/PhysRevB.107.L140411](https://doi.org/10.1103/PhysRevB.107.L140411).
- [41] L. Seabra, T. Momoi, P. Sindzingre and N. Shannon, *Phase diagram of the classical Heisenberg antiferromagnet on a triangular lattice in an applied magnetic field*, Phys. Rev. B **84**, 214418 (2011), doi:[10.1103/PhysRevB.84.214418](https://doi.org/10.1103/PhysRevB.84.214418).
- [42] D. Yamamoto, G. Marmorini and I. Danshita, *Quantum phase diagram of the triangular-lattice xxz model in a magnetic field*, Phys. Rev. Lett. **112**, 127203 (2014), doi:[10.1103/PhysRevLett.112.127203](https://doi.org/10.1103/PhysRevLett.112.127203).
- [43] A. V. Chubukov and D. I. Golosov, *Quantum theory of an antiferromagnet on a triangular lattice in a magnetic field*, Journal of Physics: Condensed Matter **3**(1), 69 (1991), doi:[10.1088/0953-8984/3/1/005](https://doi.org/10.1088/0953-8984/3/1/005).
- [44] A. V. Chubukov and T. Jolicoeur, *Order-from-disorder phenomena in Heisenberg antiferromagnets on a triangular lattice*, Phys. Rev. B **46**, 11137 (1992), doi:[10.1103/PhysRevB.46.11137](https://doi.org/10.1103/PhysRevB.46.11137).
- [45] B. Kleine, E. Müller-Hartmann, K. Frahm and P. Fazekas, *Spin-wave analysis of easy-axis quantum antiferromagnets on the triangular lattice*, Zeitschrift für Physik B Condensed Matter **87**, 103 (1992), doi:[10.1007/BF01308264](https://doi.org/10.1007/BF01308264).

- [46] Q. Sheng and C. L. Henley, *Ordering due to disorder in a triangular Heisenberg antiferromagnet with exchange anisotropy*, Journal of Physics: Condensed Matter **4**(11), 2937 (1992), doi:[10.1088/0953-8984/4/11/020](https://doi.org/10.1088/0953-8984/4/11/020).
- [47] R. Moessner and S. L. Sondhi, *Ising models of quantum frustration*, Phys. Rev. B **63**, 224401 (2001), doi:[10.1103/PhysRevB.63.224401](https://doi.org/10.1103/PhysRevB.63.224401).
- [48] M. A. Nielsen and I. L. Chuang, *Quantum Computation and Quantum Information*, Cambridge University Press, doi:[10.1017/CBO9780511976667](https://doi.org/10.1017/CBO9780511976667) (2010).
- [49] Y. Da Liao, H. Li, Z. Yan, H.-T. Wei, W. Li, Y. Qi and Z. Y. Meng, *Phase diagram of the quantum ising model on a triangular lattice under external field*, Phys. Rev. B **103**, 104416 (2021), doi:[10.1103/PhysRevB.103.104416](https://doi.org/10.1103/PhysRevB.103.104416).
- [50] S. R. White and R. M. Noack, *Real-space quantum renormalization groups*, Phys. Rev. Lett. **68**, 3487 (1992), doi:[10.1103/PhysRevLett.68.3487](https://doi.org/10.1103/PhysRevLett.68.3487).
- [51] M. C. Gutzwiller, *Correlation of electrons in a narrow s band*, Phys. Rev. **137**, A1726 (1965), doi:[10.1103/PhysRev.137.A1726](https://doi.org/10.1103/PhysRev.137.A1726).
- [52] W. Metzner and D. Vollhardt, *Analytic calculation of ground-state properties of correlated fermions with the gutzwiller wave function*, Phys. Rev. B **37**, 7382 (1988), doi:[10.1103/PhysRevB.37.7382](https://doi.org/10.1103/PhysRevB.37.7382).
- [53] X. Deng, L. Wang, X. Dai and Z. Fang, *Local density approximation combined with gutzwiller method for correlated electron systems: Formalism and applications*, Phys. Rev. B **79**, 075114 (2009), doi:[10.1103/PhysRevB.79.075114](https://doi.org/10.1103/PhysRevB.79.075114).
- [54] N. Lanatà, H. U. R. Strand, X. Dai and B. Hellsing, *Efficient implementation of the gutzwiller variational method*, Phys. Rev. B **85**, 035133 (2012), doi:[10.1103/PhysRevB.85.035133](https://doi.org/10.1103/PhysRevB.85.035133).
- [55] T. Ayrál, T.-H. Lee and G. Kotliar, *Dynamical mean-field theory, density-matrix embedding theory, and rotationally invariant slave bosons: A unified perspective*, Phys. Rev. B **96**, 235139 (2017), doi:[10.1103/PhysRevB.96.235139](https://doi.org/10.1103/PhysRevB.96.235139).
- [56] C. Schilling, *The quantum marginal problem*, <https://arxiv.org/abs/1404.1085>.
- [57] X.-D. Yu, T. Simnacher, N. Wyderka, H. C. Nguyen and O. Gühne, *A complete hierarchy for the pure state marginal problem in quantum mechanics*, Nature Communications **12**(1), 1012 (2021), doi:[10.1038/s41467-020-20799-5](https://doi.org/10.1038/s41467-020-20799-5).